

**Best Available  
Copy  
for all Pictures**

AD-776 591

MOLDING OF ORIENTED SHORT-FIBER  
COMPOSITES. II. FLOW THROUGH  
CONVERGENT CHANNELS

Lloyd A. Goettler

Monsanto Research Corporation

Prepared for:

Office of Naval Research  
Advanced Research Projects Agency

March 1974

DISTRIBUTED BY:

**NTIS**

National Technical Information Service  
U. S. DEPARTMENT OF COMMERCE  
5285 Port Royal Road, Springfield Va. 22151

## DOCUMENT CONTROL DATA - R &amp; D

(Security classification of title, body of abstract and indexing annotation must be entered when the overall report is classified)

1. ORIGINATING ACTIVITY (Corporate author)		2a. REPORT SECURITY CLASSIFICATION	
Monsanto Research Corporation		Unclassified	
		2b. GROUP	
3. REPORT TITLE			
Molding of Oriented Short-Fiber Composites II. Flow Through Convergent Channels			
4. DESCRIPTIVE NOTES (Type of report and inclusive dates)			
5. AUTHOR(S) (First name, middle initial, last name)			
Lloyd A. Goettler			
6. REPORT DATE		7a. TOTAL NO. OF PAGES	7b. NO. OF REFS
March, 1974		57	14
8a. CONTRACT OR GRANT NO.		9a. ORIGINATOR'S REPORT NUMBER(S)	
N00014-67-C-0218		HPC 70-130	
b. PROJECT NO.			
c.		9b. OTHER REPORT NO(S) (Any other numbers that may be assigned this report)	
d.			
10. DISTRIBUTION STATEMENT			
Approved for public release; distribution unlimited			
11. SUPPLEMENTARY NOTES		12. SPONSORING MILITARY ACTIVITY	
		Office of Naval Research Washington, D. C.	
13. ABSTRACT			
<p>Superior mechanical properties can be attained in a short fiber composite by utilizing the flow in transfer or injection molding to align the fibers into the direction of highest stress. This is best accomplished in an elongational flow field, such as occurs in a converging channel. A model is derived to describe the changes in orientation distribution resulting from this flow. We investigated the effects of the geometric, material, and processing variables on the orientation parameters of this model, the resulting orientation level and the tensile modulus of molded rods.</p>			

Reproduced by  
NATIONAL TECHNICAL  
INFORMATION SERVICE  
U S Department of Commerce  
Springfield VA 22151

14 KEY WORDS	LINK A		LINK B		LINK C	
	ROLE	WT	ROLE	WT	ROLE	WT
transfer molding						
plunger molding						
elongational flow						
tensile modulus						
composite						
fiberglass						
epoxy						
converging flow						
fiberglass						
fabrication						
fiber alignment						
fiber suspensions						
viscosity						
orientation angle						
..						

HPC 70-130

ITEM A002

MOLDING OF ORIENTED SHORT-FIBER COMPOSITES

II. FLOW THROUGH CONVERGENT CHANNELS

by

Lloyd A. Goettler

March 1974

MONSANTO/WASHINGTON UNIVERSITY ASSOCIATION  
HIGH PERFORMANCE COMPOSITES PROGRAM  
SPONSORED BY ONR AND ARPA  
CONTRACT NO. N00014-67-C-0218, ARPA ORDER 876  
ROLF BUCHDAHL, PROGRAM MANAGER

MONSANTO RESEARCH CORPORATION  
800 NORTH LINDBERGH BOULEVARD  
ST. LOUIS, MISSOURI 63166

iii.

## FOREWORD

The research reported herein was conducted by the staff of Monsanto/Washington University Association under the sponsorship of the Advanced Research Projects Agency, Department of Defense, through a contract with the Office of Naval Research, N00014-67-C-0218 (formerly N00014-66-C-0045), ARPA Order No. 876, ONR contract authority NR 356-484/4-13-66, entitled, "Development of High Performance Composites."

The prime contractor is Monsanto Research Corporation. The Program Manager is Dr. Rolf Buchdahl (Phone 314-694-4721).

The contract is funded for \$7,000,000 and expires 30 June, 1974.

## Introduction

Injection and transfer molding afford an economical means to fabricate short fiber reinforced composites on a large volume basis. The hydrodynamic forces generated by the flow deformation of the fiber-melt suspension affect the composite structure by changing the fiber orientation, fiber distribution, fiber length, fiber loading, fiber wetting and void content of the molding compound. This paper describes how the fiber orientation induced by the flow can be quantitatively controlled by the selection of flow geometry and material characteristics in order to optimize the mechanical performance of molded parts. If left uncontrolled, unfavorable orientation patterns may cause the loss of 75% of the potential stiffness and over 80% of the tensile strength. For this reason, the commercial molding industry has not been able to fully exploit the cost advantages of flow fabrication of short fiber composites. Previous treatments of this problem have been only descriptive (1,2,3).

For two reasons we will herein consider only the stiffness property of moldings. In the first place, a distinct advantage is obtained for stiffness applications by aligning the fibers in the direction of stress, whereas the ultimate properties of short fiber composites cannot in practice be made to exceed those of a quasi-isotropic distribution (4). In many engineering applications, materials with a high stiffness are preferred to those exhibiting a high tensile strength and moderate stiffness.

Secondly, stiffness is a direct measure of fiber orientation for the molded samples discussed in this report. Although the ultimate tensile properties depend critically upon the angular deviation of anisotropic material structural elements from the direction of stress, they are strongly affected as well by the other five primary structural variables mentioned earlier. Stiffness, on the other hand, shows a weaker dependence upon fiber distribution and wetting and the presence of minor voidage. Since the local concentration of reinforcement does not vary widely in flow moldings (5), and since the length of glass fibers need only exceed 1/32" in order to realize 90% of the continuous fiber stiffness in plastic matrices, the Young's modulus has a one-to-one correspondence with the fiber orientation pattern in most thermoset moldings. (Use of shorter fibers might invalidate this conclusion for thermoplastic systems.)

Certainly a myriad of geometrical shapes can be encountered in a mold design. Five basic right prisms that differ in form relative to the gate placement are identified in Figure 1. Many straight sections can be approximated by one of these arrangements. In addition, a complete study of the effects of cavity geometry on fiber orientation would have to involve the gate size relative to the cavity dimensions, nonparallel wall sections and curved channels, including bends and tees. If the effect of each of these sections on the orientation in the molding compound entering that section were known, the complete orientation distribution in a molded part could be synthesized by joining the necessary elements together to at least approximate the overall geometry. However, that is beyond the scope of this paper.



Instead only elements of Type I are considered. They occur frequently not only as a part component but also as the runner system of a mold or the flow channel of an extruder. In addition, a circular cross-section is adopted for symmetry in order to simplify the description and analysis of orientation. Since it is usually desirable to align the fibers along the long direction of the part for optimum mechanical reinforcement, our aim is to investigate the fiber "orientability" in different molding materials and to relate this to the degree of axial alignment possible in the channel geometry shown in Figure 2. Such information will directly apply to the design of molds for transfer or injection molding of fiber-reinforced thermosets, where the converging channel can be either incorporated into the runner system or made an integral part of the molded piece. The extension of our results to thermoplastic resins will also be considered.

#### Rheology of Concentrated Fiber Suspensions

Depending upon the viscosity of the suspending fluid (or matrix resin) fiber suspensions at concentrations exceeding five volume percent fiber (5v/o) exhibit either a Bingham or a pseudoplastic behavior. The former occurs when the resin viscosity is less than about 5,000 poise, and comprises a plug flow through uniform channels with all shear occurring in a thin ( $< .5\text{mm}$ ) layer of pure resin at the wall (6). In this condition, which applies in general to thermosetting matrices, there is no effect of shearing flows on the fiber orientation distribution. As the viscosity increases (and probably also as shear rate increases), the fiber core begins

to shear at its edges, giving a flatly curved velocity profile corresponding to a pseudoplastic fluid with a low flow index of  $1/3 - 1/3$  (7). Since thermoplastic matrices typically exhibit viscosities of  $10^4 - 10^5$  poise at their processing temperatures, some shear orientation of fiber into the direction of flow will occur near the walls.

However, the predominant mechanism for aligning fibers is an elongational flow field. One example of pure elongation, a completely irrotational flow, is the stretching of a film. Rod-like particles imbedded in the medium will orient toward a steady state in which they are aligned along the direction of stretch. A purely elongational field also results when highly concentrated fiber suspensions in a low viscosity matrix flow through a converging channel.

Takserman-Krozer and Ziabicki (8) relate the rotation of a rigid ellipsoid in very dilute suspension to an extentional velocity gradient in uniform extension

$$\dot{\theta}_1 = - \frac{3}{4} \lambda \left( \frac{dv_1}{dx_1} \right) \sin 2\theta_1 \quad (1)$$

$$\dot{\phi}_1 = 0 \quad (2)$$

where  $\theta_1$  is the co-latitude or polar angle and  $\phi_1$  the longitude or projected angle in the  $x_2$ - $x_3$  plane in a spherical coordinate system based on  $x_1$  as the polar axis.

$x_1$  is directed along the streamline through the center of the ellipsoid.

$\lambda$  is a shape coefficient  $\frac{r^2 - 1}{r^2 + 1}$  related to the eccentricity,  $r$ , of the ellipsoid. It approaches unity for both rods and ellipses when the particle axis ratio exceeds 10.

$v_1$  is the signed axial velocity component being negative in converging flows.

The assumption that the particles are rigid is valid for our short fiberglass composites. However, particle interactions in highly loaded composites ( $> 10$  v/o fiber) play a large role in determining orientation behavior and cannot be neglected.

A rheological model developed by Ericksen (9) for transversely isotropic fluids extends the applicability of Equation (3) by allowing  $\lambda$  to be a phenomenological material constant that is not tied to the particle shape by may assume values both greater and less than unity. The degree of fiber interaction which depends upon the physical constitution of the system, including fiber length and concentration, determines the value of  $\lambda$ . Since large values of  $\lambda$  result in faster fiber rotations and a higher degree of alignment, it will be called the "orientability" parameter.

### Fiber alignment in flow through a tapered tube

The system geometry is presented in Figure 2. Fiber position and fiber orientation are each described in terms of spherical coordinate systems, with primed angles used to denote the former. The system shown in the figure uses subscripts of unity to indicate that the polar axis is along  $x_1$ , the principal direction of the flow. This is taken as the cone axis for describing fiber position and as the streamline through the center of the fiber for describing fiber orientation. The  $x_2$  direction is defined as being perpendicular to  $x_1$  and lying in the plane of an axial slice through the channel.  $x_3$  is then orthogonal to this plane. Equivalent spherical coordinate systems with polar axes along the  $x_2$  and  $x_3$  directions may also be defined. The angles of these are identified by subscripts 2 and 3 respectively.

The rate of elongation in material flowing through this channel with slip at the wall is a function of axial position

$$v_1 = - \frac{Q}{2\pi x_1^2 (1 - \cos \alpha)} \quad (3)$$

$$\dot{\epsilon}_{11} \equiv \frac{dv_{x_1}}{dx_1} = \frac{Q}{\pi x_1^3 (1 - \cos \alpha)} \quad (4)$$

There is no dependence on distance from the wall since shearing is absent for these fluids. The superimposed shear flow that would be present with a thermoplastic melt is neglected in this work, which will deal with a low viscosity B-staged thermosetting system. However, Modlen (10) has shown that even when it is present the concurrent shear in an elongational flow has a comparatively small effect on the fiber orientation distribution.

Equation (4) is valid as long as the angle of convergence is sufficiently small so that stagnant regions do not exist at the exit of the converging channel and flow instabilities are absent. These conditions are met except for possible instabilities at the cone exit for the experiments described below. The equation predicts that the material will see a large change in elongation rate as it moves down the channel at a constant volumetric flow rate,  $Q$ . This is shown graphically in Figure 3 for a  $6^\circ$  taper. However, the variation over a half-fiber length ( $\leq 1/8"$ ) is only 20% under the most unfavorable conditions, so that Equation (1) is locally valid.

To allow for the variation in  $\dot{\epsilon}_{11}$ ,  $\theta_1$  in Equation (1) is viewed as the derivative following the motion. Then

$$\dot{\theta}_1 = \frac{D\theta_1}{Dt} = v_1 \frac{d\theta_1}{dx_1} \quad (5)$$

for steady flow through the converging channels. Substituting Equation (5) for  $\dot{\theta}_1$ , Equation (4) for  $dv_1/dx_1$ , and Equation (3) for  $v_1$  into Equation (1) and integrating over  $x_1$  yields the result

$$\tan \theta_1 = c x_1^{3\lambda} \quad (6)$$

or

$$\tan \theta_1 = c' A^{\frac{3}{2}\lambda}$$

where  $c, c'$  are arbitrary constants.

$A$  is the area of the spherical surface of radius  $x_1$  that is transcribed by the boundaries of the channel. It is closely approximated by the cross-sectional area of the channel at position  $x_1$ . A similar result has been obtained by Takano (6) for planar hyperbolic flows.

In the derivation,  $\theta_1$  has been interpreted as the changing orientation taken on by a single fiber as it traverses the converging channel. In applying the analysis to the description of fiber orientation distributions in molded parts, however, the Eulerian rather than the Lagrangian viewpoint is assumed.  $\theta_1(x_1)$  then represents the axial variation in orientation displayed at any one instant by equivalent fibers all following the same flow path through the channel.

Equation (6) then describes the angular dependence of  $\theta_1$  on  $x_1$  along a given streamline, which is identified by the value of  $c$  corresponding to the initial orientation at the streamline when it enters the conical channel. Thus (6) becomes

$$\frac{\tan \theta_1}{\tan \theta_1^0} = \left( \frac{x_1}{x_1^0} \right)^{3\lambda} = \left( \frac{A}{A^0} \right)^{\frac{3}{2}\lambda} \quad (7)$$

Some typical changes in  $\theta_1$  predicted by this equation are illustrated in Figure 4. Large values of  $\lambda$  result in faster rotations. The S-shape of the curves predicts that the highest rate of rotation of the fibers occurs when they are aligned at  $45^\circ$  to the streamline. An initial transverse  $90^\circ$  orientation represents an unstable state of equilibrium. Similarly, the approach to absolute alignment along the streamline is also very slow. Proper design of a convergence would allow for reasonably good alignment without going to excessively large area changes. In a mold design the small outlet diameter would conform to the dimensions of the molded part, and the larger upstream area that would be required for orientation might pose an economic burden in terms of mold cost, machine capacity, and material loss unless it, too, could be incorporated into the part.

Since the orientation across the channel will not generally be uniform, some measure of the overall orientation for the entire cross-section must be devised to compare with the measured stiffness of the molded rods. This can be done either

pragmatically through the use of an "average" angle  $\bar{\theta}_1$ , or more elegantly by the use of orientation distribution functions.

Let  $\rho(\theta_1, t)$  be a probability distribution function indicating the time-dependence of  $\theta_1$  in a Lagrangian sense. Then the change in  $\rho$  is given by

$$\frac{D\rho}{Dt} = - \frac{\partial}{\partial \theta_1} \left( \rho \frac{D\theta_1}{Dt} \right) + \mathcal{L} \frac{\partial^2 \rho}{\partial \theta_1^2} \quad (8)$$

where  $\mathcal{L}$  is a degradative diffusion coefficient that can be used to represent randomizing processes such as Brownian motion in the case of very small particles or an eddy effect in these fiber suspensions. For simple fiber models it can be taken equal to zero. When  $\mathcal{L}$  is zero, substitution of Equations (1) and (5) into (8) gives, at steady state

$$v_1 \frac{\partial \rho}{\partial x_1} = \frac{\partial}{\partial \theta_1} \left[ \frac{3}{4} \rho \lambda \left( \frac{dv_1}{dx_1} \right) \sin 2\theta_1 \right]$$

or

$$\frac{\partial \rho}{\partial x_1} = \frac{3}{2} \frac{\lambda}{x_1} \left( 2\rho \cos 2\theta_1 + \frac{\partial \rho}{\partial \theta_1} \sin 2\theta_1 \right) \quad (9)$$

This first-order partial differential equation describes the change in the orientation distribution away from a known initial distribution that must be measured at one end of the converging section.



## Materials

The molding compounds used in the experimental study were composed of a low molecular weight epoxy resin of the epichlorohydrin/bisphenol A type\* that was cured with methylenedianiline\*\* at 30 phr. After blending the resin at 60°C with chopped E-glass\*\*\* (240 fibers per bundle, coated with an epoxy-compatible silane binder), the formulation was kept at temperature for 30 min. followed by 18 hours at room temperature to yield a B-stage in which 45-50 percent of the epoxide groups were reacted into a predominantly linear structure. In this condition the molding compound is non-tacky at room temperature and exhibits the following desirable characteristics on molding at 95°C:

- i) a viscosity of about 5,000 poise that is sufficiently high to produce some shearing apart of the fiber bundles in flow through small orifices while keeping shear forces in the converging section to a negligible level.
- ii) a constant viscosity for a period of 5 min. during which flow occurred.
- iii) a high exotherm following the latent period that raised the internal temperature to give a full cure in 30 min.

---

\* Epon 828, Shell Chemical Company.

\*\* 4,4'-methylenedianiline, Eastman Organic Chemicals.

\*\*\*Type CS-308A, Johns-Manville Company.

## Experimental

The molding compound was preheated in an RF oven to the mold temperature of 95°C and was then manually formed into a plug and placed in the pot of a plunger-type transfer molding press. Hydraulic pressure on a 1-1/2 inch diameter ram caused flow through a 1/2" x 1/8" runner into the cavity system shown in Figure 2. Fill rate was controlled by adjusting ram travel speed through a flow control on the hydraulic line. The cavity consists of three sections: an upstream uniform channel of 1-1/4" diameter and 3/4" length to receive the incoming material through a small gate from the runner, a converging section and an attached rod 4" in length.

The function of the upper section is to orient the fibers in an initial position largely transverse to the flow axis. This results from the increase in cross-sectional area and deceleration of the fluid that occurs in passing through a small gate into a large cavity, as described previously (3). The parabolic shape of the pattern comprising a transverse core with longitudinal alignment along the edge of the channel results both from a wall effect and from the radiating shape of the flow field at the gate leading into the upper section. Reorientation of the fibers in an elongational flow can be studied in the conical section. Once the initial orientation pattern was established, the wall effect did not further influence the fiber rotation measured in the cone.

The half-angle,  $\alpha$ , can be varied from  $6^\circ$  to  $90^\circ$  by fitting conically-shaped inserts made of an aluminum-filled epoxy tooling resin into a cylindrical cut-out in the steel mold. The diameter,  $d$ , of rods attached to the conical section can also be varied by the use of tooling resin inserts. Figure 5 shows these inserts in place in the mold block.

Since shear is not transferred to the fibers during flow through a uniform channel, the orientation produced in the converging section tends to be maintained throughout the straight rod cavity. Rods of diameter  $1/4"$ ,  $3/8"$  and  $1/2"$  have been molded and tested for tensile modulus in an Instron testing machine. Specimen elongation used in the calculation of modulus was measured with a strain gauge extensometer attached to the specimen. There was some variance introduced in the measurements by the limited point contact of the extensometer clips against the cylindrical surface. By repeat measurements on a single sample it was found that the measurement standard deviation was  $.14 \times 10^6$  psi, or 5%. In contrast, the overall precision involving reproducibility of molding conditions as well as measurement error was  $0.21 \times 10^6$  psi or about 8%.

A longitudinal section of a molding cut through the axis is shown in Figure 6. The fiber alignment is seen to change from transverse to axial in passing through the converging channel. The fiber orientation patterns are made visible by etching the polished surface with hydrofluoric acid to pit the fiber bundles, and then filling these with a dye. Methods for characterizing the fiber orientation and subsequently utilizing these measurements to calculate the polar

angle  $\theta_1$  as a function of coordinate position are described elsewhere.(11) It is also shown there that the bundle patterns represent the local mean orientation of individual fibers in a small neighborhood of about .01 inch diameter. In this work the measurements of the changing planar angle  $\phi_3$  along the axial direction in a single plane of the conical section are employed to determine the orientation parameter  $\lambda$  .

When molding compound is injected at high speed into a closed mold, various phenomena such as jetting, air entrapment and compaction can influence the orientation distribution in the molded part. Since one aim of this work is to relate such orientation, as manifested in the stiffness, to the rotational "orientability" of the fibers, a method of operation was devised to avoid these anomalous effects. This required the capability to produce flow through the mold after the cavity had been filled and the melt subjected to a compaction pressure. A small outflow orifice that could be opened or blocked by the pivot shown in Figure 7 was installed in the downstream end of the rod for this purpose. Aside from its academic interest, flow through the mold and out this orifice represents actual flows that might occur in the upstream section of a complex molding containing a pinched region.

In a typical molding sequence, the cavity pressure would instantaneously increase and the flow rate decrease when the cavity initially fills and outflow extrusion through the orifice commences at a lower rate. The volumetric flow rate during outflow is monitored from a recorder plot of ram position as a function of time.

The cavity pressure is simultaneously recorded from a pressure transducer located under the head of an ejector pin. Outflow continues until a purge of at least one rod volume occurs to set up steady-state conditions. Then the pivot arm is swung into position over the orifice, flow stops abruptly and the cavity pressure registers another small sharp increase to the stagnant level under which the epoxy cures. The time for these operations is kept to less than five minutes so that the interpretation of flow phenomena is not complicated by a progressively increasing cure state. Simulated recorder outputs to illustrate the procedure are shown in Figure 8.

#### Test of the Orientation Model

Measurements of progressive rotation along a straight streamline at constant  $\phi_1'$  and  $\theta_1' = 3^\circ$  in the converging section were made to test the validity of Equation (6). Angles measured in the polished plane, such as that shown in Figure 6 are  $\phi_3$ , the angle the fiber projection in a longitudinal plane cut through the flow axis makes with the streamline. These are related to the polar angle  $\theta_1$  by

$$\cos \phi_1 \tan \theta_1 = \tan \phi_3. \quad (9)$$

The equation derives from geometrical relationships. Since integration of Equation (2) predicts that  $\phi_1$  is constant,

$$\tan \theta_1 \propto \tan \phi_3.$$

Substitution into Equation (6) yields

$$\tan \phi_3 = C'' x_1^{3\lambda} \quad (10)$$

where  $C''$  is just another arbitrary constant and Equation (10) has the same form as the model, Equation (6), for polar orientation. Consequently, verification of (10) also verifies (6), and the  $\lambda$ -values determined from the planar analysis are the material constants previously described.

Some measured angles on two different streamlines in the conical section are plotted as  $\ln \tan \phi_3$  vs  $\ln x_1$  in Figure 9. As predicted by Equation (10), these data can be correlated by a straight line. The slope, which is equal to  $3\lambda$ , is independent of  $\theta_1'$ , the position of the streamline in the conical channel. Since the elongation rate,  $\dot{\epsilon}_{11}$ , varies with  $x_1$ , we see that the orientability parameter  $\lambda$  is indeed a constant, independent of the deformation conditions. The vertical positioning of the two lines reflects the different initial orientations for the two streamlines, because of their different positioning in the conical cross-section. The one at larger  $\theta_1$  is near the wall, and enters the curved region of the upstream orientation profile. However, in both cases the slope, equal to  $3\lambda$ , is the same, which indicates the independence of  $\lambda$  from  $\theta_1$  and also the absence of any wall effect upon the orientation process.

#### Definition of Variables

In Table I are listed the dimensionless variables which may be expected to influence the fiber orientation. The first four of these are geometric variables. Of these, the area reduction ratio is the most important since that variable appears explicitly in the mathematical model for  $\theta_1$ , Equation (7). All of the other parameters listed in the table might be important through their possible effect

on the orientability parameter,  $\lambda$ . Variables 5 and 6 are entirely processing-controlled, but 7, 8 and 9 are determined in part by the material formulation. In particular, fiber aggregation results not only from the hardness of the binding on the fiber bundles used, but also from the degree of shear to which the suspension is subjected, as in flowing through small gates. Matrix viscosity is a dual function of the degree of B-stage and the molding temperature. Voids can be present either initially in the molding compound, or can be introduced, or removed, during processing. Variables 10 and 11 are clearly material variables. It should be noted that the flow rate,  $Q$ , and matrix viscosity,  $\eta$ , are likely combined in their effect through the Reynold's Number, indicating that they act through an inertial effect. The limit of all flows to low Reynold's Numbers of order of magnitude of unity indicates that inertial effects are not important and consequently that these will probably not be important variables.

The orientation distribution at the end of the conical section joining to the rod, and hence the rod stiffness, depend on some considerations besides the orienting behavior discussed above.

1. As Equation (7) predicts, the orientation at the outlet of the core depends upon the upstream level of orientation. However, correlation of  $\theta_1^\circ$  for the moldings produced shows that this predominantly transverse orientation does not change by more than several degrees over all the moldings made with the same material. Average values are tabulated in Table II.

2. Flow disturbances at the juncture of the cone and the rod may be caused by the abrupt direction change of the streamlines to bring them into parallelism, material relaxation due to the cessation of stretching forces, or instabilities leading to melt fracture caused by the very high elongation rates at the cone exit.
3. There could be a significant wall effect due to the smaller size of either the channel diameter/fiber length ratio or the channel diameter/shear layer ratio in rods of small diameter. In the latter case, the higher shear stresses may cause the shearing to spread from the lubricating resin layer into the fiber network.
4. The core of the fluid, which is highly transverse, may be in an unstable equilibrium that is not disturbed by molding into the large (1/2" diameter) rods. A residual transverse core in the rods would result. Although this effect has been observed, it does not seem to be prevalent enough to degrade the rod stiffness.

## Results

The large number of independent variables, as listed in Table I, precludes a statistically systematic investigation. However, experiments were run at two or three levels of most of the variables in order to deduce the main effects.

1. Void Fraction. In all of the experiments reported here, the void content present during the flow was low ( $< 5\%$ ; usually  $< 2\%$ ). This condition was produced by any one or more of the following conditions: i) low fiber content, (ii) short fibers, or



(iii) flow occurring under pressure after compaction, as described above. This condition represents the true orientation response of the material, and the variable of void fraction will not be considered further.

2. Flow rate, viscosity and fiber aggregation. Measured values of the orientability,  $\lambda$ , for 40 v/o of 1/8" fibers as a function of flow rate are presented in Figure 10. The melt pressure during flow through a 1/8" diameter outflow orifice varied from 2000 to 8000 psi. The  $\lambda$ -values were determined from the slope of a least squares line through a plot of measured  $\ln \tan \phi_3$  against  $\ln x_1$  similar to Figure 9. Each point represents a single molding except for repeated measurements at .85 in<sup>3</sup>/min to obtain a measure of the standard deviation. The data show no statistically significant variation of  $\lambda$  with  $Q$ , and the mean  $\lambda$  of 0.47 is indicated by the horizontal line. Independence of  $\lambda$  from the flow rate is to be expected since  $Q$  acts through its effect on  $\epsilon_{11}$ , and  $\lambda$  was previously shown to be independent of that parameter. The runs reported involved ingate (above the large upstream section) diameters of both 1/8" and 1/2" diameter. This caused slight observable changes in the degree of dispersion of the fiber bundles in the molding, but such changes had no effect upon the orientability of the molding compound. The range of flow rates covered is reasonable for the flow of such a filled molding compound through small (1/8" diameter) orifices under a melt pressure at the ram of up to 10,000 psi.

Moldings of 1/2" diameter rods (area reduction ratio,  $A^*/A = 6.25$ ) made under these conditions were tested for tensile modulus,  $E$ . The data plotted in Figure 11 against flow rate again indicate no dependence. Each data point on this graph represents an individual sample. The filled-in points were molded through a 1/8" diameter ingate; all others used a 1/2" diameter gate. Again, as in the case of  $\lambda$ , there is no difference in stiffness attributable to differing degrees of fiber aggregation (dispersion) or to fiber damage with the smaller gate.

Also indicated on this graph by the shapes of the data points are differences in viscosity level. This is a normalized viscosity based on laminar flow through a series of uniform conduits and conical sections. The treatment in the Appendix shows that in a fixed geometry  $\eta \propto \Delta P/Q$ . Since the main flow resistance was in the outflow orifice,  $\Delta P$  in this case is taken as the internal cavity pressure. The 25-fold range in viscosity reported in Figure 11 was produced by variations in the B-stage of the molding compared either in its manufacture or in extensive preheating. There is no effect on the stiffness of the molded rods. It can be concluded from this that the orientation pattern and the orientability itself are independent of viscosity. Such a result agrees with the previous contention that the effects of  $Q$  and  $\eta$  can be combined in a Reynold's Number. Then if one of them had no effect on  $\lambda$ , the other must not by necessity either.

3. Cavity pressure. Higher cavity pressures might be expected to cause a reduction in voidage and an increase in fiber wet-out. That this at least does not affect the modulus of 1/2" rods molded from 40 v/o of 1/8" fiberglass in epoxy at cavity pressures up to 7,000 psi is shown in Figure 12.
4. Geometrical size parameters. When the rod diameter is reduced to 3/8", the area reduction ratio increases accordingly to 11.1. Under these conditions the measured stiffness  $2.55 \times 10^6$  psi surprisingly shows no increase. A further reduction to 1/4" diameter ( $A^0/A = 25$ ) causes only a slight increase in E to  $2.82 \times 10^6$  psi. In both cases the loading is 40 v/o of 1/8" fiberglass. Clearly these results do not follow the prediction of the orientation model that the orientation varies with the  $\frac{3}{2} \lambda$  power of  $A/A^0$ . One might suspect that this anomalous behavior is caused by the concurrent reductions in the parameters channel diameter/fiber length and channel diameter/shear layer. This point will be covered in the discussion.
5. Fiber length and  $l/d$ . The diameters of all the K-filament glass used in this work is about .50 mil. Consequently, changes in fiber length correspondingly change the aspect ratio. At 40 v/o of 1/4" fiber, molded with outflow under pressure to eliminate voidage, a rod stiffness of  $2.3 \times 10^6$  psi is obtained for 1/2" rods, and  $3.3 \times 10^6$  psi for 1/4" rods.

The rather large value for the 1/4" rod is attributed to a wall interaction with the long fibers ( $d/\ell = 1$ ) in the rod.

Shorter fibers were also studied, in the form of milled glass (35 v/o of Owens Corning type 701B 1/32" milled fiber in the usual epoxy formulation). Over a very broad range of flow rates from 0.5 to above 20. in<sup>3</sup>/min the modulus of 3/8" molded rods was constant at  $2.0 \times 10^6$  psi. The lower level of stiffness can be attributed to the lower fiber content and to less efficiency in load transfer, due to the very short fiber length in this case. The fact that the stiffness is not as low as it should seem for such short fibers (avg.  $\ell/d = 25$ ) can be explained by a rather low initial angle  $\bar{\theta}_1^\circ$  of  $60^\circ$ , leading to a higher than usual alignment in the rods.

6. Fiber concentration. The experiments at a lower concentration level of 25 v/o for the 1/8" fibers were performed differently in that the outflow orifice was kept shut during the entire molding sequence, permitting no flow under a compaction pressure. With the 40 v/o material an anomalous dependence of orientability and rod stiffness on elongation rate was attributed to high voidage in the flowing melt under these conditions (12). That such behavior does not occur at the lower loading is evidenced by the data in Figures 13 and 14. The mean values are 0.77 for  $\lambda$  and  $1.84 \times 10^6$  psi for E.

7. Angle of convergence. No significant effects of this parameter were detected for the moldings conducted with flow under pressure. However, for cases in which the orientability is a function of elongation rate, the angle of convergence will play a major role (12).

The above data are summarized in Table III. The predicted average angles appearing in this table result from the application of Equation (7) to the measured upstream average angle  $\theta_1^\circ$ . Predicted stiffnesses result from a plot of measured stiffness versus measured average angle determined for various types of flow moldings (12).

### Discussion

The values of the orientability parameter,  $\lambda$ , measured for fiber-filled epoxy molding compounds in this study deviate severely below the level of unity expected for two limiting classes of materials. These are specifically a suspension of long fibers in which the concentration is sufficiently low that there are no fiber-fiber interactions, and materials in which the fibers rotate in accord with the deformation of a homogeneous continuum. In this latter simple approach, the orientation is directly related to the draw ratio, which can be equated to  $A^\circ/A$  in our terminology. Such analyses have been applied to model composites by Modlen (10) and to crystallites in polymers by Ward (13).

Our measured orientabilities are clearly low because of the fiber interaction, which was to be expected. The inapplicability of the continuum analyses to the practical fabrication of composite

materials becomes evident when one considers that its results correspond to the case for noninteracting fibers. The higher value of  $\lambda$  for the less concentrated (25 v/o) suspension results from the lower degree of interaction and consequently higher mobility of the fibers.

The data summarized in Table III for 1/8" fibers clearly indicate that the predictions of the model, Equations (6) or (7) using the measured values of  $\lambda$ , for the degree of orientation in small rods are not met. Very good agreement is obtained for rods of 1/2" diameter, for which the area reduction ratio ("draw ratio") is only 6.25. The constant level of rod stiffness at increasing area reductions could, in principle, be attributed to either flow instabilities that occur in the regions of high  $\dot{\epsilon}_{11}$  at small diameter core outlets (see Fig. 3) or augmented shear in the wall regions of small channels.

Shear, unlike extension, is a rotational flow. In dilute suspensions, the fibers rotate at a nonuniform angular velocity which is greatest at a position 90° to the flow direction and slowest when the fibers are aligned along that direction. The net effect is thus that shear favors alignment of the fibers into the direction of flow, the longitudinal dimension of the rods in this case (14). In more concentrated suspensions, the fiber rotations may be slower and, in fact, if the fiber interaction is high enough, a stable orientation at some angle to the flow direction might occur, the magnitude of the angle depending upon the material constants (9). Takano (6) has reported improvements in orientability when the matrix viscosity in a fiber suspension is sufficiently high that some level

of shear occurs in elongational flows. We substantiate that result by observations of fiber position in very small runners, where shear becomes significant. Only when the degree of alignment into the flow direction becomes very high would it be reasonable that the transient nature of fiber rotations in shear might disturb an established orientation distribution. At average alignments of  $20^{\circ}$ - $25^{\circ}$ , such a situation does not exist in the molded rods and the limitation on alignment must not be the result of shearing.

Flow instabilities, on the other hand, are observable in the orientation patterns in molded rods. These are documented elsewhere (12). Some possible causes for such disturbances have been mentioned earlier, but the high elongation rates at the cone outlet probably lead to inherent material instability. This phenomenon has been well documented in the literature dealing with plastics extrusion and spinning. Very high elongation rates cause rupture of the material, leading to extrudate fracture, but instabilities are detected even for low convergence angles and flow rates.

An instability phenomenon that is solely dependent on rate of elongation is independent of the size of the mold. Under the conditions of constant angles, geometric ratios, and time-to-fill, the elongation rate is independent of the scale-up of a mold cavity. This conclusion, together with the disappointing experimental results, implies that average polar orientations greater than about  $20^{\circ}$ - $25^{\circ}$  will not be feasible in flow-molded thermoset composites.

A possible exception might be at very low fiber contents where the elasticity of the fiber network does not dominate over the resin contribution to flow behavior.

Since thermoplastic resins are generally processed at higher viscosity levels ( $\geq 10^4$  poise), the contribution of shear might impart stability to the flows and also aid in improving the fiber alignment. Alignment would also be favored by the build-up of a frozen skin of shear-aligned material at the cold wall during flow. However, injection molding cycles are usually shorter than for transfer molding. The resulting higher deformation rates in flow might be detrimental to the fiber alignment process.

It should finally be noted that in any commercial mold of either the injection or transfer type, the conservation of mold size will favor the use of short converging sections with steep convergence angles. For the same flow rate, these give rise to higher elongation rates than the  $6^\circ$  angle used in this study. However, these results may be expected to apply as long as the maximum  $\dot{\epsilon}_{11}$  (at the cone exit) does not greatly exceed that corresponding to the flow rates and geometry of our study.

### Conclusions

A mathematical model employing a single parameter termed the orientability was derived and applied to fiber rotations in a fiber-filled epoxy molding compound flowing through a conically converging channel. Extensional forces of the flow tend to align



the fibers into the axial direction. The degree of alignment should be a function of the area reduction, which is in effect a draw ratio, but instabilities limit the attainable average polar angles to 20-25°. The orientability parameter is determined by fiber interactions and takes on a value less than that predicted from affine transformations based on the effective draw ratio.

A modulus of  $2.5-3.3 \times 10^6$  psi in rods attached to the conical section is nevertheless possible by flow alignment techniques. This compares with  $1.5 \times 10^6$  psi for a typically end-gated piece without the converging section to produce the proper fiber orientation. The results are directly applicable to transfer molding of reinforced thermosets and, in principle, to other systems.

#### Acknowledgment

The author wishes to express his gratitude to Mr. D. J. Morotz and to Miss A. M. Gordon for their assistance in the experimental phases of this study.

This research was supported by the Advanced Research Projects Agency of the Department of Defense and was monitored by the Office of Naval Research under Contract No. N00014-67-C-0218.

Table I

Variables Affecting Fiber Orientation (in dimensionless form)

1. Area reduction ratio,  $A^0/A = (x_1^0/x_1)^2$
2. Angle of convergence,  $\alpha$  , degrees
3. Channel diameter/fiber length,  $d/\ell$
4. Channel diameter/shear layer,  $d/d_s$
5. Flow (fill) rate,  $Q$ , in<sup>3</sup>/min - see 8.
6. Cavity pressure,  $P/P_{atm}$
7. Fiber aggregation
8. Matrix viscosity,  $\eta$  , poise  $N_{Re} = \frac{4\rho Q}{\pi D\eta}$
9. Void content,  $v/o$
10. Fiber concentration, volume percent (v/o)
11. Fiber length/fiber diameter,  $\ell/d_f$

Table II

Upstream Orientation Angle,  $\bar{\theta}_1^\circ$

---

<u>Material</u>	<u><math>\bar{\theta}_1^\circ</math> degrees</u>
1/8" Fibers CS308A, 40 v/o	63.
1/8" Fibers CS308A, 25 v/o	69.
1/32" Milled Fibers, Type 701B, 35 v/o	60.

Table III

## Data Summary

$$\alpha = 6^\circ$$

Fiber	Content v/o	Rod diam in	A°/A	$\lambda$	E 10 <sup>6</sup> psi	$\bar{\theta}_1^\circ$ degrees	$\bar{\theta}_1$ pred in rod, deg.	E pred 10 <sup>6</sup> psi	% dev. in E meas.
1/8" CS308A	40	1/2	6.25	.47	2.5	63	28.	2.6	-4.
		3/8	11.1	↓	2.6	↓	20.	3.8	-32.
		1/4	25.	↓	2.8	↓	11.	4.3	-35.
	25	3/8	11.1	.77	1.8	69	9.	3.0	-40.
	40	1/2	6.25	-	2.3	-			
		1/4	25.	-	3.3	-			
1/32" milled	35	3/8	11.1	-	2.0	60			

## References

1. Woebcken, W., Modern Plastics, 40, 146 (Dec. 1962).
2. Fuccella, D., SPE Retec, Cleveland, Oct. 1971.
3. Goettler, L. A., Modern Plastics, 48, 140 (April 1970).
4. Lavengood, R. E., Polymer Eng. and Sci., 12, 48 (1972).
5. Goettler, L. A., Monsanto/Washington Univ. ONR/ARPA Assoc. Report HPC 72-149, SPE Antec 1973 p. 559.
6. Takano, M., to be published.
7. Thomas, D. P. and R. S. Hagan, 21st SPI Reinforced Plastics Division Meeting, 1966, Section 3-C.
8. Takserman-Krozer, R. and A. Ziabicki, J. Poly. Sci., A1, 491 (1963).
9. Ericksen, J. L., Kolloid Z., 173(2), 117 (1960).
10. Modlen, G. F., J. Mater. Sci., 4, 283 (1969).
11. Goettler, L. A., Monsanto/Washington Univ. ONR/ARPA Assoc. Report HPC 72-151, also 25th SPI Composites Div. Mtg., 1970, Section 14A.
12. Goettler, L. A., Monsanto/Washington Univ. ONR/ARPA Assoc. Report HPC 72-150.
13. Ward, I. M., Proc. Phys. Soc., 80, 1176 (1962).
14. Goldsmith, H. L. and S. G. Mason, in Eirich, F., ed., "Rheology," Vol. 4, Academic Press, N. Y., 1967, pp. 86-250.

### List of Figures

1. Possible straight channel geometries relative to the gate position.
2. Channel geometry;  $D = 1.25$  inches,  $d = .25; .375$ , or  $.50$  inches.
3. Elongation rate variations in a  $6^\circ$  cone.
4. Typical variations in  $\theta_1$ .
5. Mold inserts.
6. Longitudinal section of a molding.
7. Latch mechanism for outflow orifice.
8. Recorder outputs and operational sequence.
9. Orientation measurements in the cone: 40 v/o  $1/4$ " fiberglass in epoxy,  $\alpha = 6^\circ$ .
10. Orientability parameter for 40 v/o of  $1/8$ " fibers;  $\alpha = 6^\circ$ .
11. Modulus of  $1/2$ " rods;  $A^\circ/A = 6.25$ ,  $\alpha = 6^\circ$ , 40 v/o of  $1/8$ " fibers.
12. Absence of pressure effect on rod stiffness;  $1/2$ " rod,  $A^\circ/A = 6.25$ ,  $\alpha = 6^\circ$ , 40 v/o of  $1/8$ " fibers.
13. Orientability parameter for a lower fiber concentration with no outflow; 25 v/o  $1/8$ " fiberglass,  $\alpha = 6^\circ$ .
14. Rod stiffness for a lower fiber concentration with no outflow; 25 v/o,  $1/8$ " fiberglass,  $\alpha = 6^\circ$ ,  $3/8$ " rod ( $A^\circ/A = 11.1$ ).

## Appendix

### Viscosity Effects

The flow model chosen is that of a Bingham plastic, with the fiber network forming a central plug, and the lubricating layer of resin at the wall constituting the sheared region. Two types of flow resistance are met in the molding operation:

- i) Poiseuille flow through straight sections
- ii) elongational flow through converging (and/or diverging) channels.

In the former case the resistance is caused solely by the shearing of the lubricating layer. In the latter, the major part of the resistance is due to the elongational deformation of the central core network and the lubricating layer may be neglected in contrast. Since the elastic properties of such a network are unknown, a purely viscous deformation is assumed. Since even the steady flow characteristics are unknown, it is further assumed to behave in a Newtonian manner.

In the case of circular symmetry, the pressure-flow rate relationships become, for the rod (R) and cone (C):

$$i) \quad \Delta P_R = \left\{ \frac{\pi r_w^4}{8\eta_R Q \Delta L} \left[ 1 - \frac{4}{3} \left( \frac{r_s}{r_w} \right) + \frac{1}{3} \left( \frac{r_s}{r_w} \right)^4 \right] \right\}^{-1}$$

where  $r_s$  = radius of the central plug

$r_w$  = radius of the channel

$\eta_R$  = viscosity of resin matrix

$Q$  = volumetric flow rate

$$\text{ii) } \Delta P_C = \frac{8Q \eta_R \Delta L}{\pi \Gamma_w F(\bar{x}, \alpha)} + \frac{2\pi^{1/2} \eta_C Q \sin^3 \alpha}{(1 - \cos \alpha)} \left[ \frac{1}{A_d^{1/2}} - \frac{1}{A_u^{1/2}} \right]$$

where  $\eta_C$  = extensional viscosity of the central core

$A_u$  = upstream area of cone

$A_d$  = downstream area of cone.

and

$$F(\bar{x}, \alpha) = 1 - \frac{4}{3} \left( 1 - \frac{t}{\bar{x}\alpha} \right) + \frac{1}{3} \left( 1 - \frac{t}{\bar{x}\alpha} \right)^4$$

where  $t$  = thickness of resin layer

$\alpha$  = half angle of the cone

Thus

$$\Delta P_C = (K_R \eta_R + K_C \eta_C) Q$$

where the  $K$ 's are geometrical constants.

The significance of these results is that for both types of flow, i) and ii)

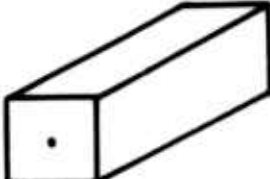
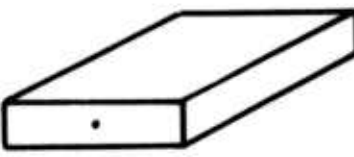
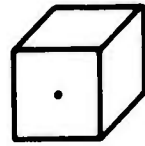

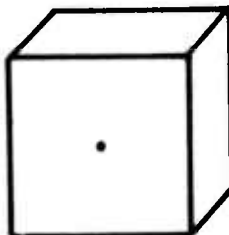
$$Q = K \frac{\Delta P}{\eta}$$

Rearranging,

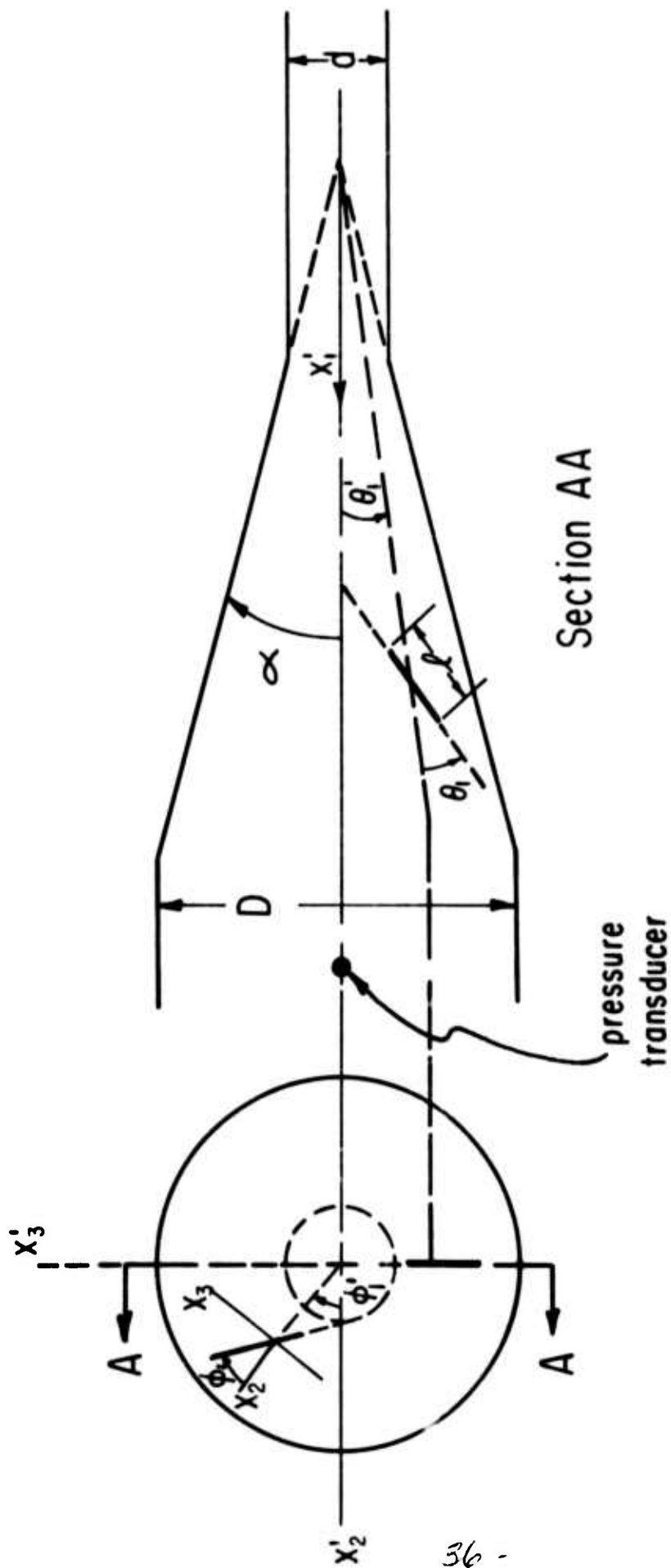
$$\frac{\eta}{K} = \frac{\Delta P}{Q} \quad \text{and } \eta \text{ is some effective viscosity.}$$

Consequently, for any specified geometry, the viscosity varies with the first power of  $\Delta P/Q$ , where  $\Delta P$  is measured over some convenient section of the flow path that includes a major flow resistance.

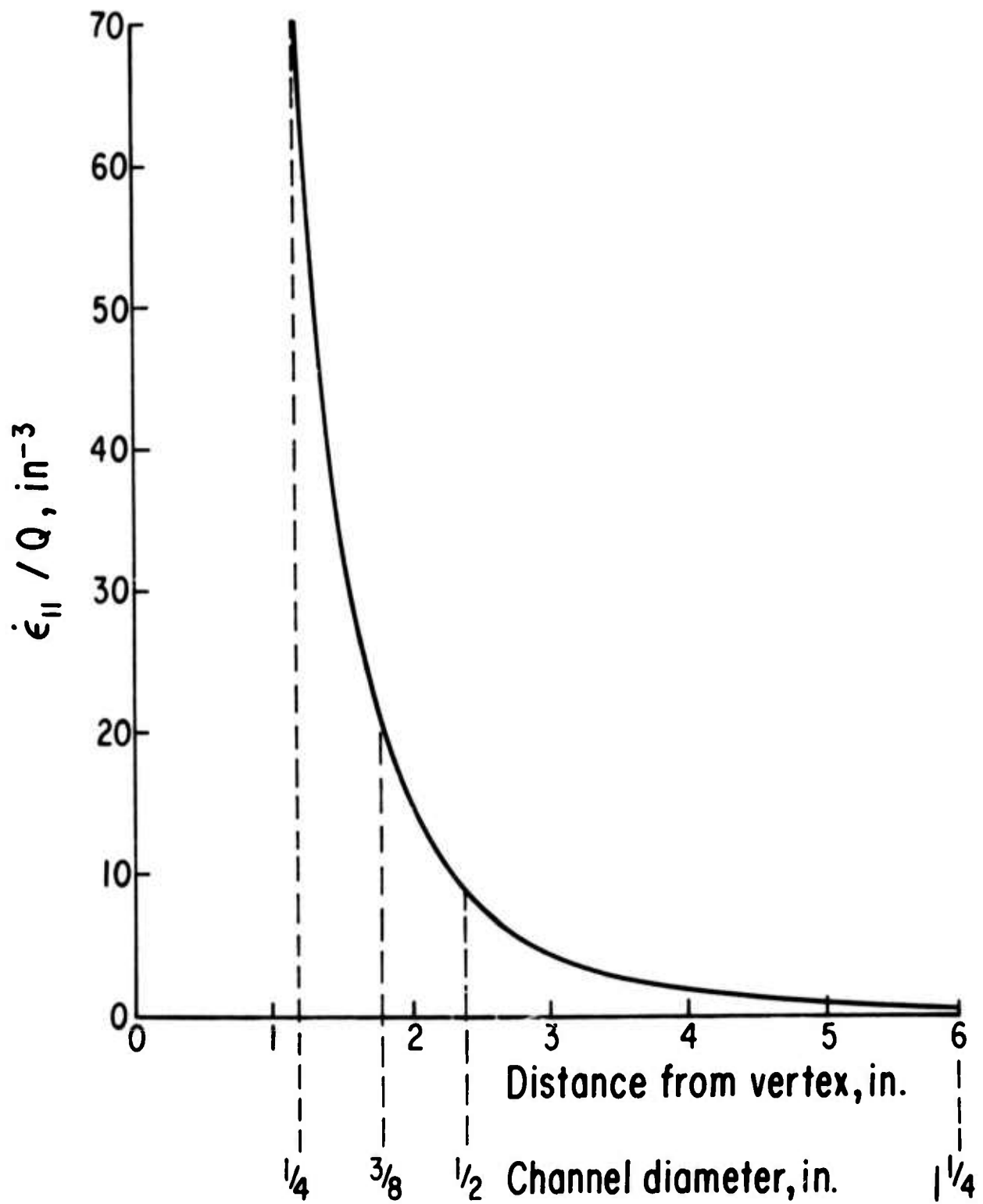


	<u>Length</u> (away from gate)	<u>Width</u>	<u>Thickness</u>	<u>Shape</u>
I.	L (long)	S (short)	S (short)	
II.	L L	L S	S } L }	
III.	L S	L S	L } S }	
IV.	S S	S L	L } S }	
V.	S	L	L	

1. Possible straight channel geometries relative to the gate position.



2. Channel geometry;  $D = 1.25$  inches,  $d = .25$ ;  $.375$ , or  $.50$  inches.



3. Elongation rate variations in a  $6^\circ$  cone.

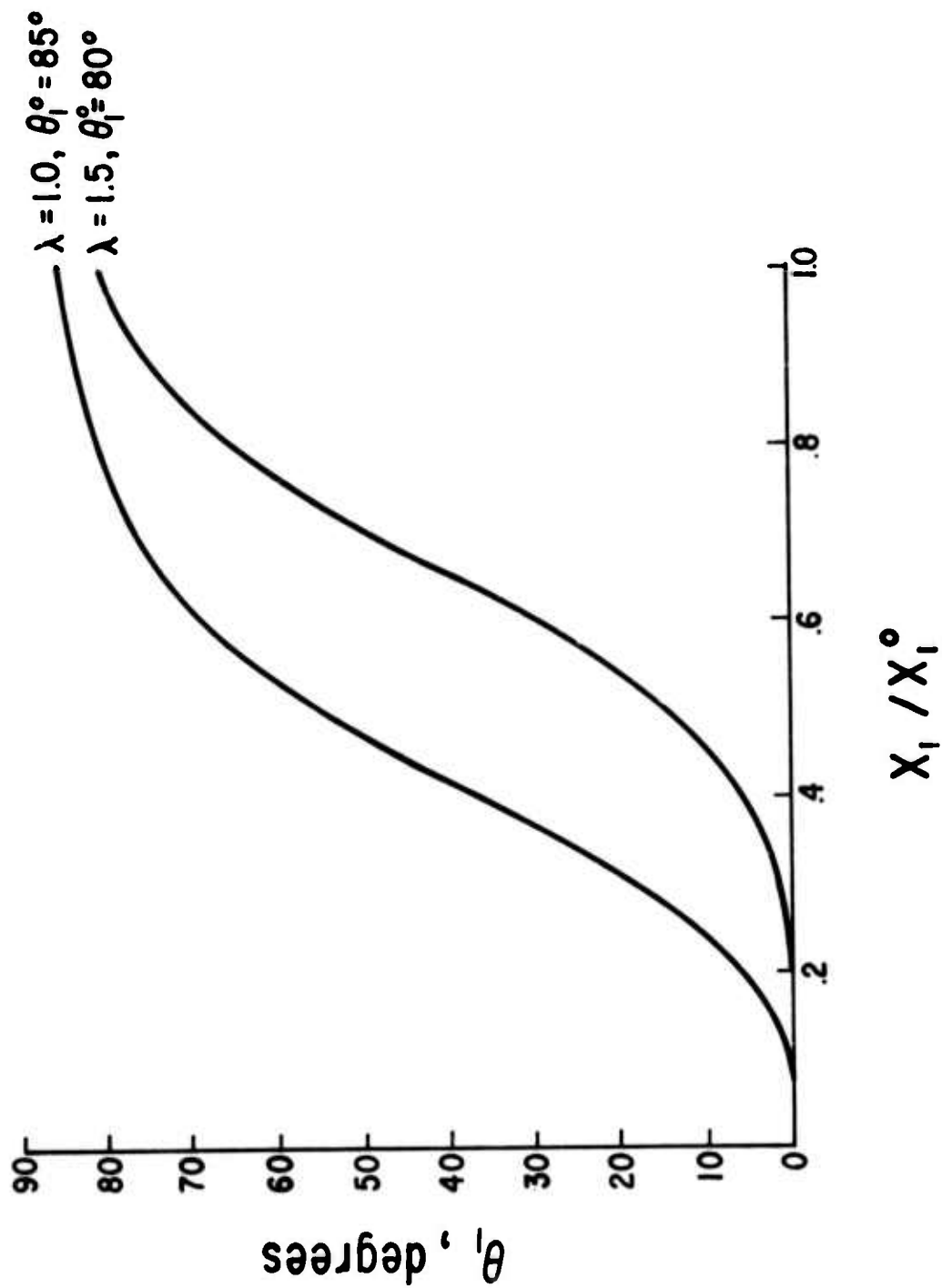
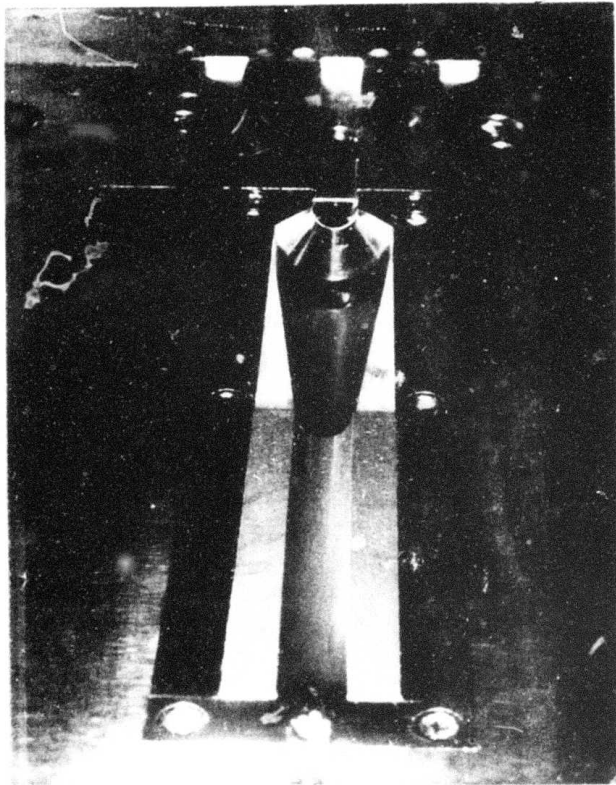
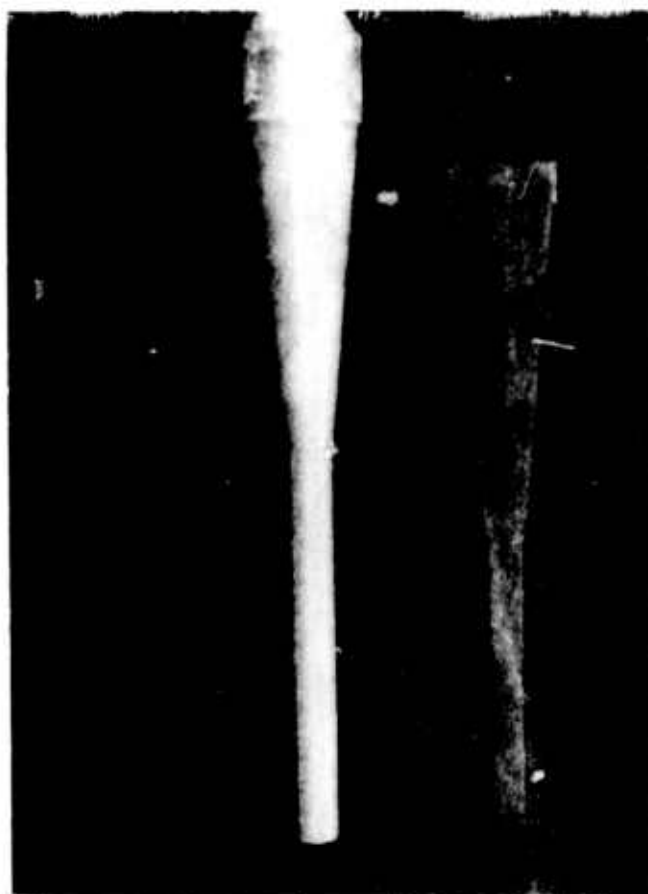


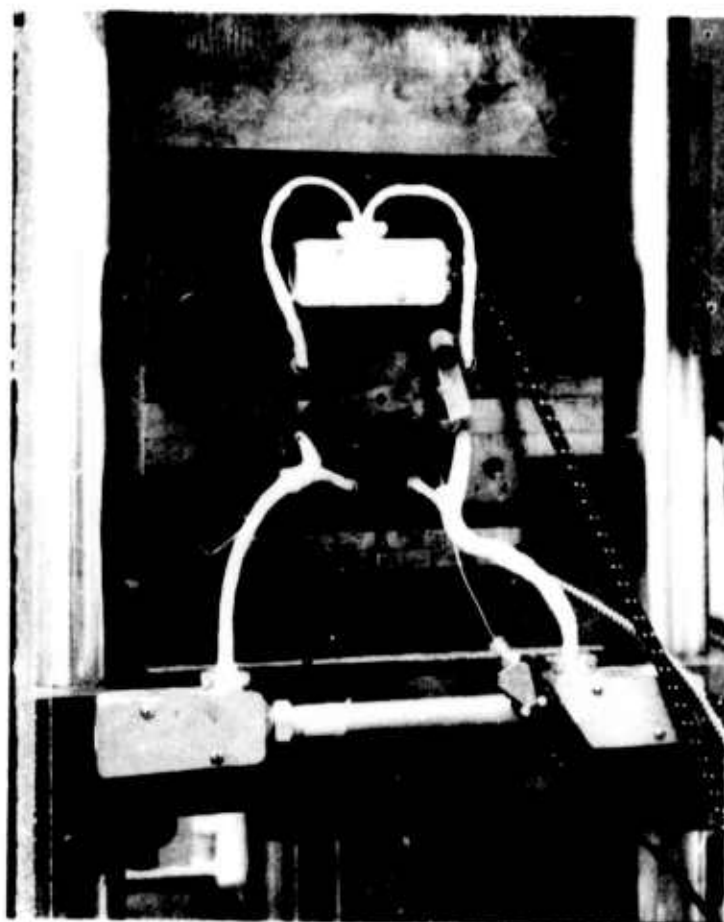
Fig. 4. Typical variations in  $\theta_1$ .



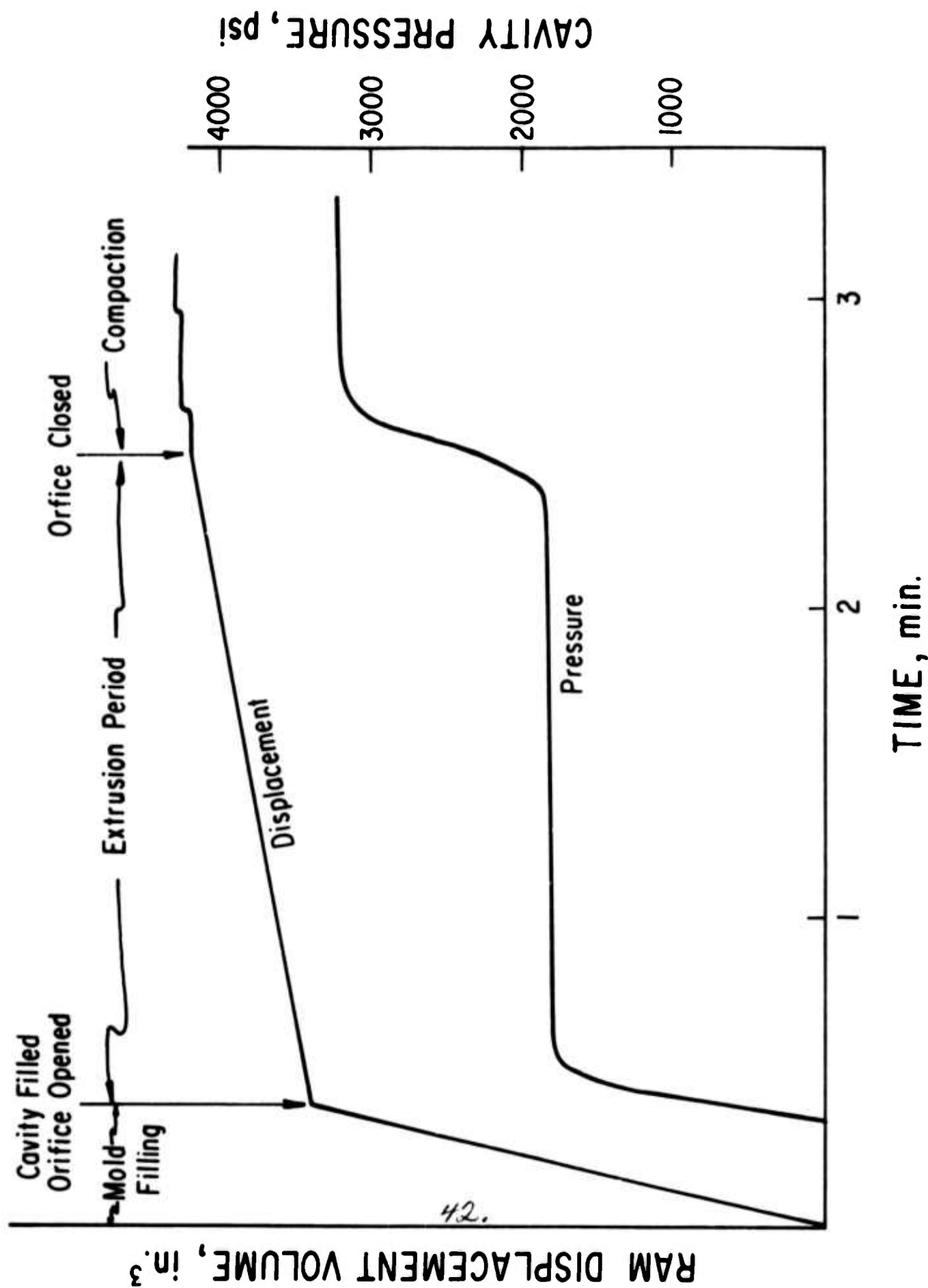
5. Mold inserts.



6. Longitudinal section of a molding.

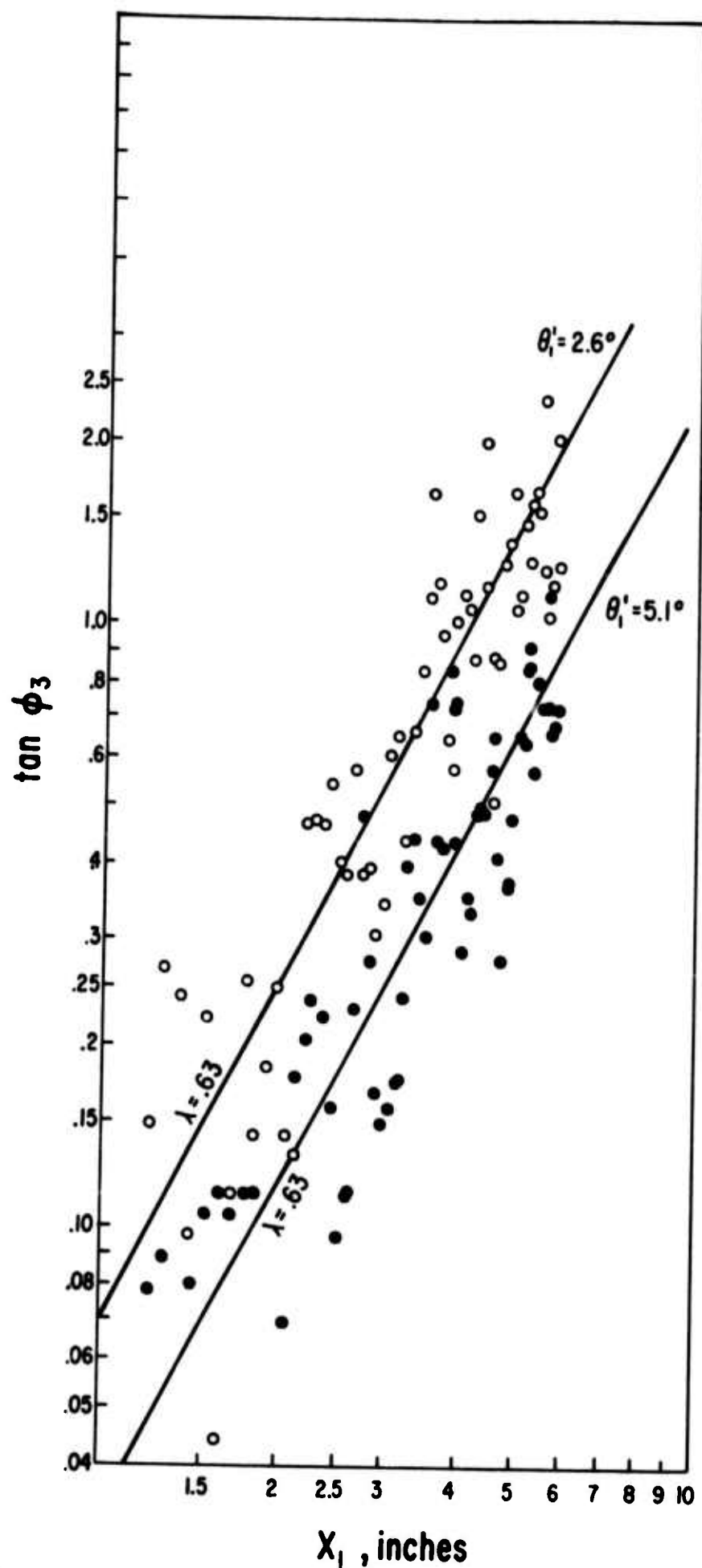


7. Latch mechanism for outflow orifice.

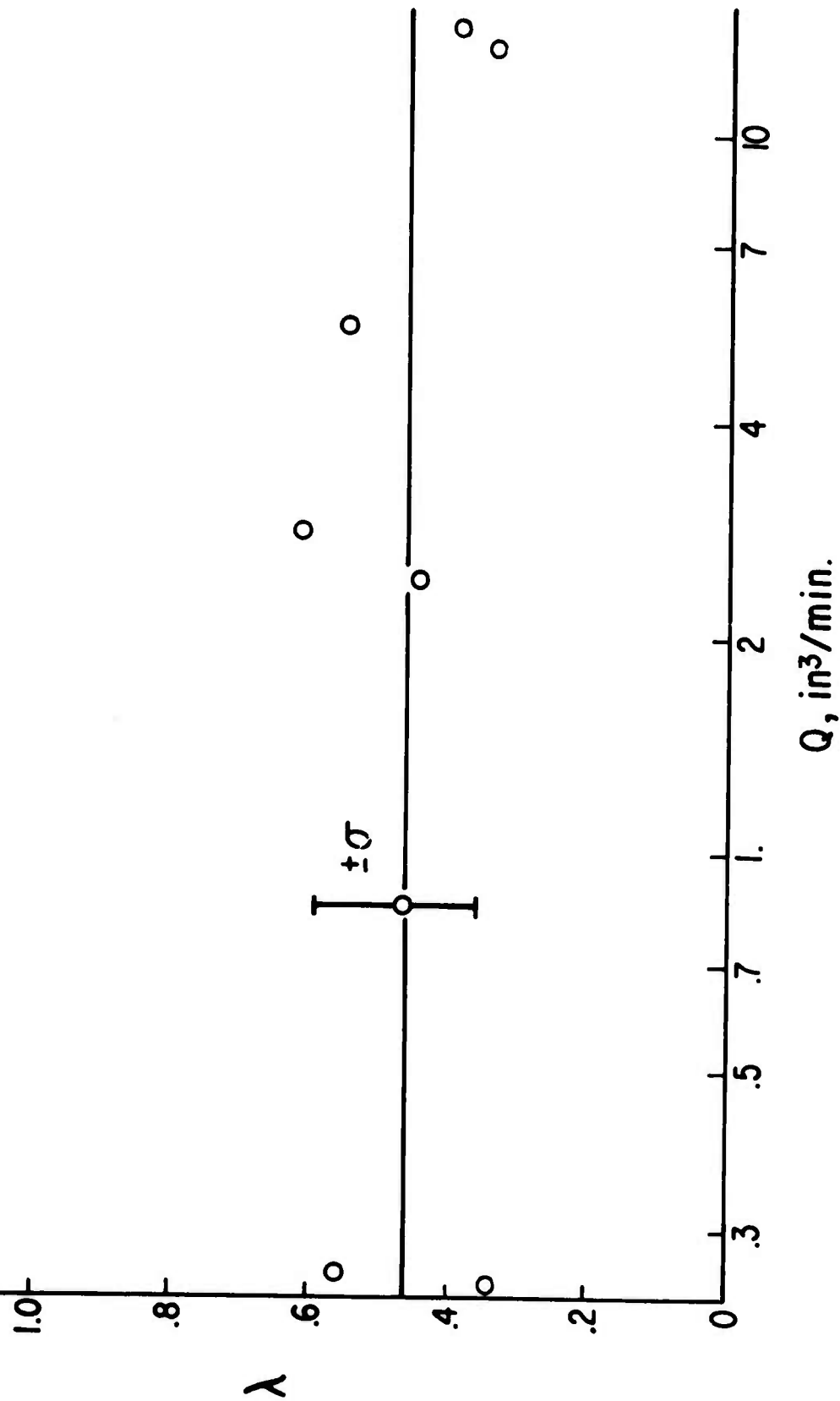


8. Recorder outputs and operational sequence.

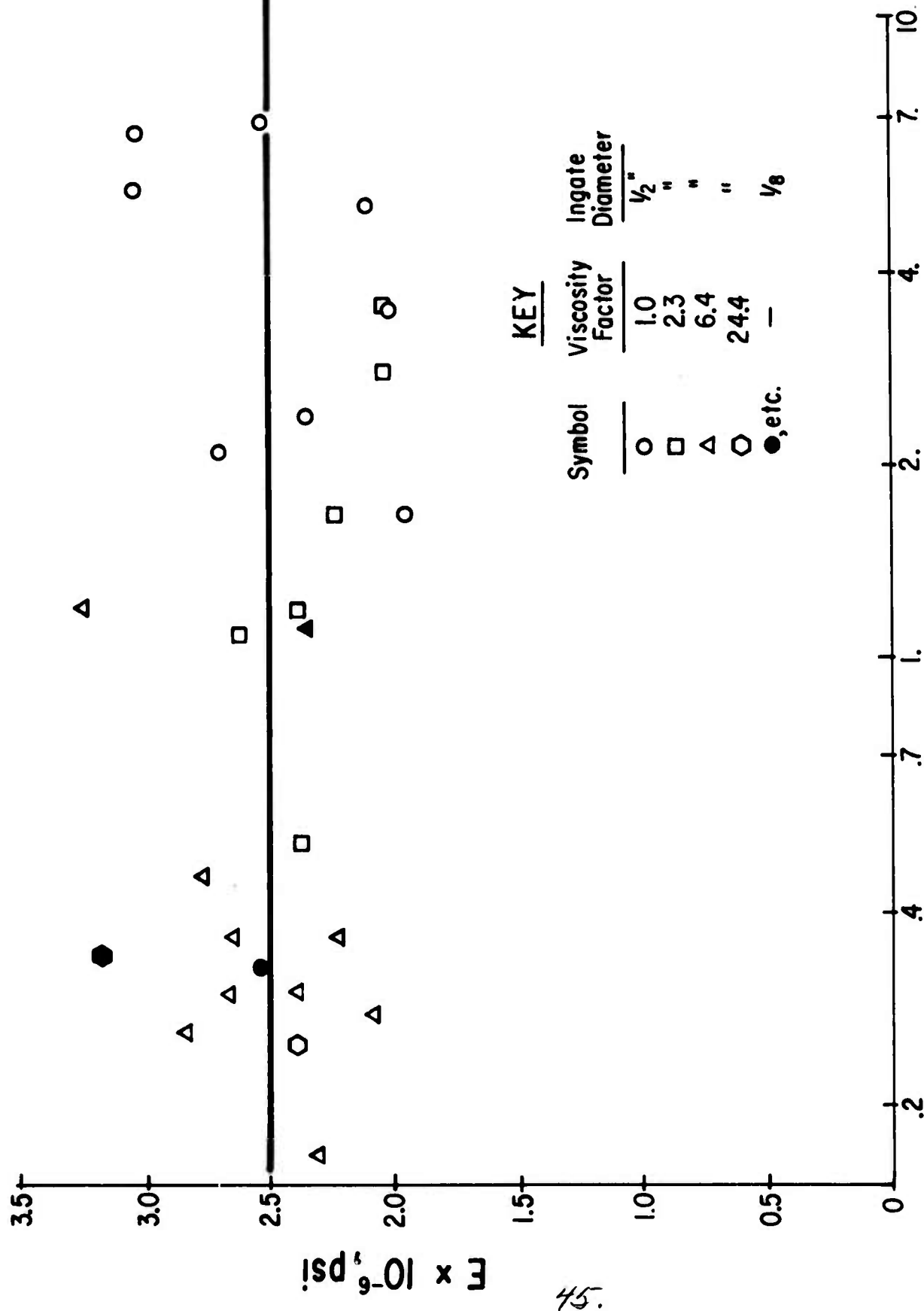




9. Orientation measurements in the cone: 40 v/o 1/4" fiberglass in epoxy,  $\alpha = 6^\circ$ .

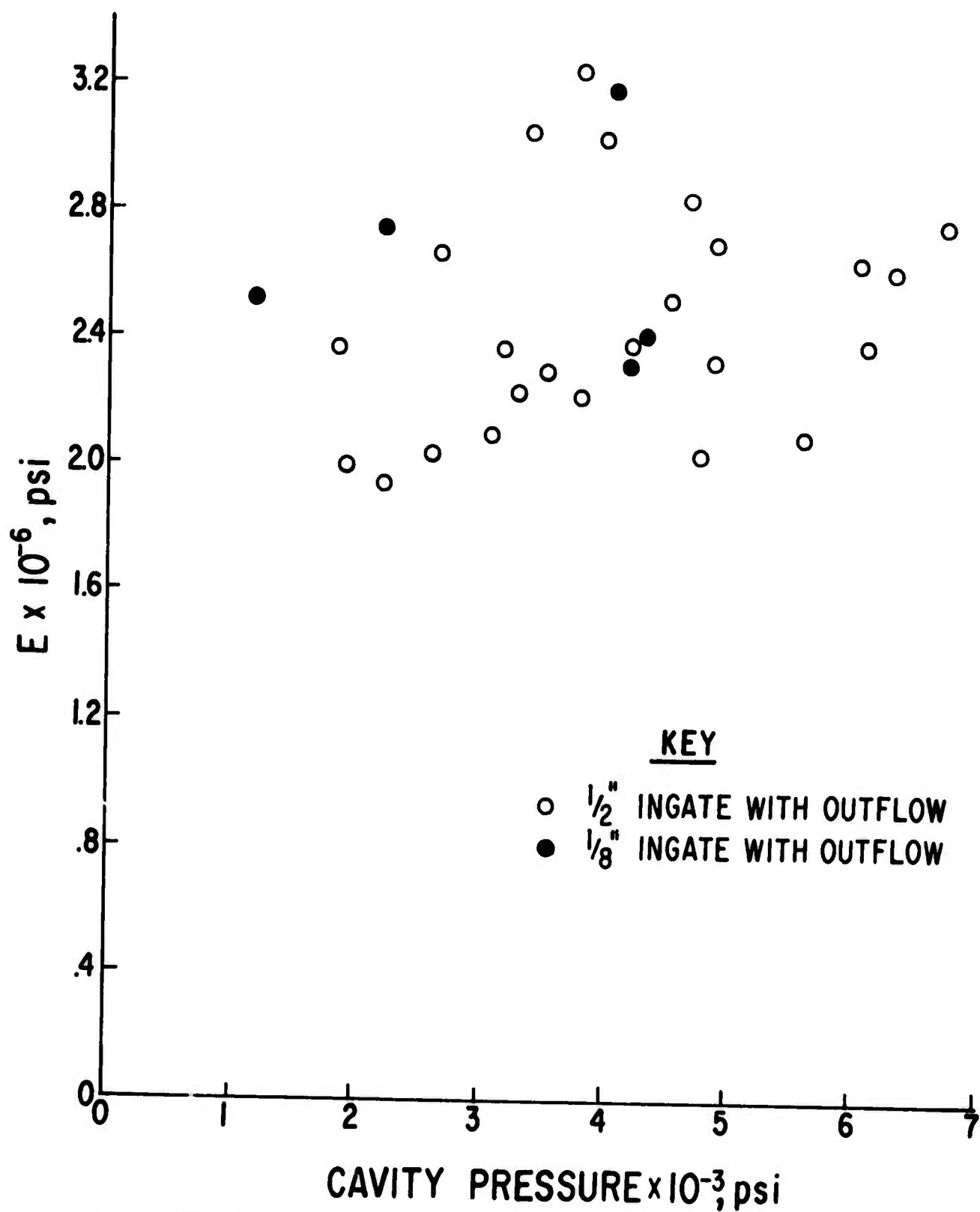


10. Orientability parameter for 40 v/o of 1/8" fibers;  $\alpha = 6^\circ$ .

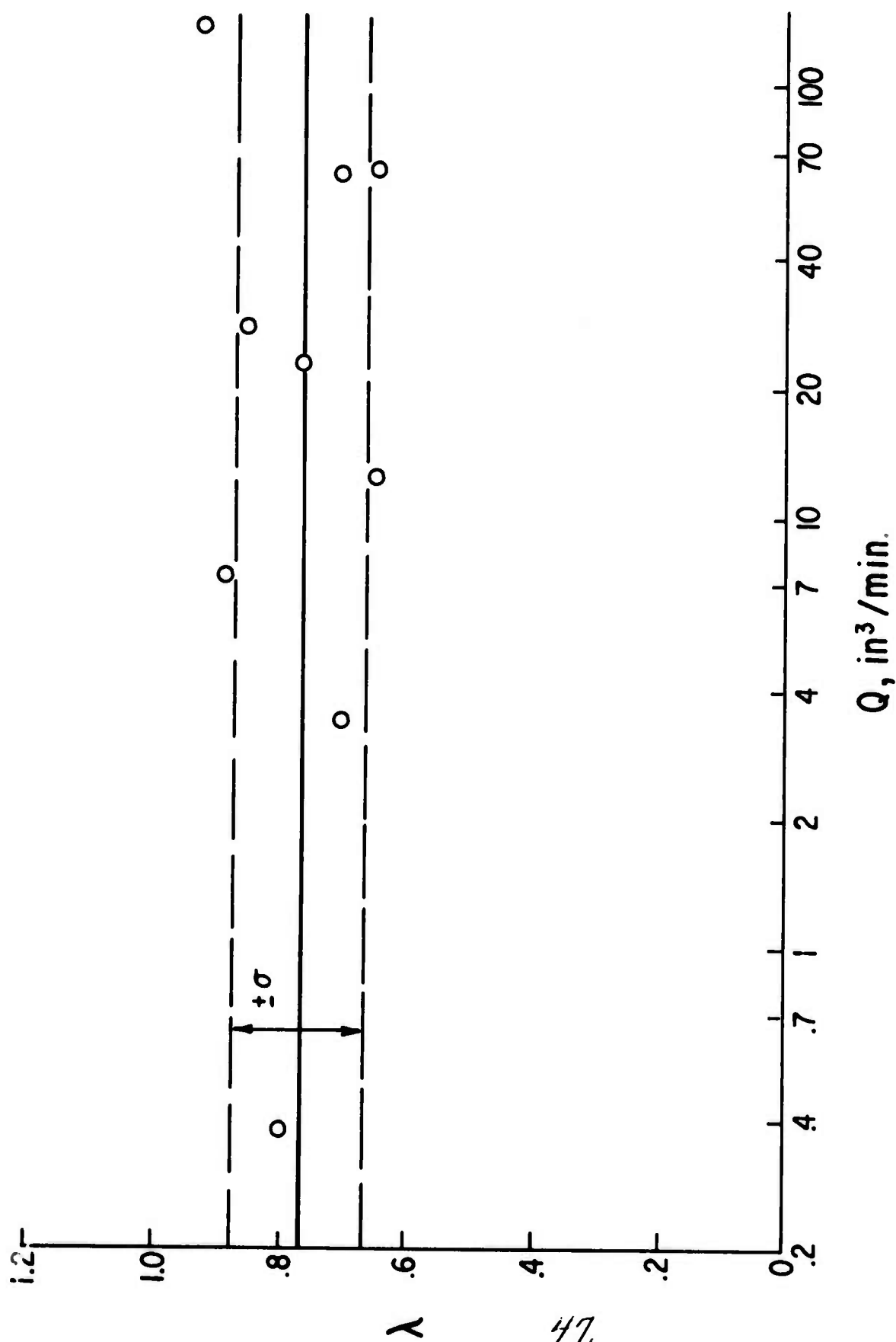


$Q, \text{ in}^3/\text{min}$

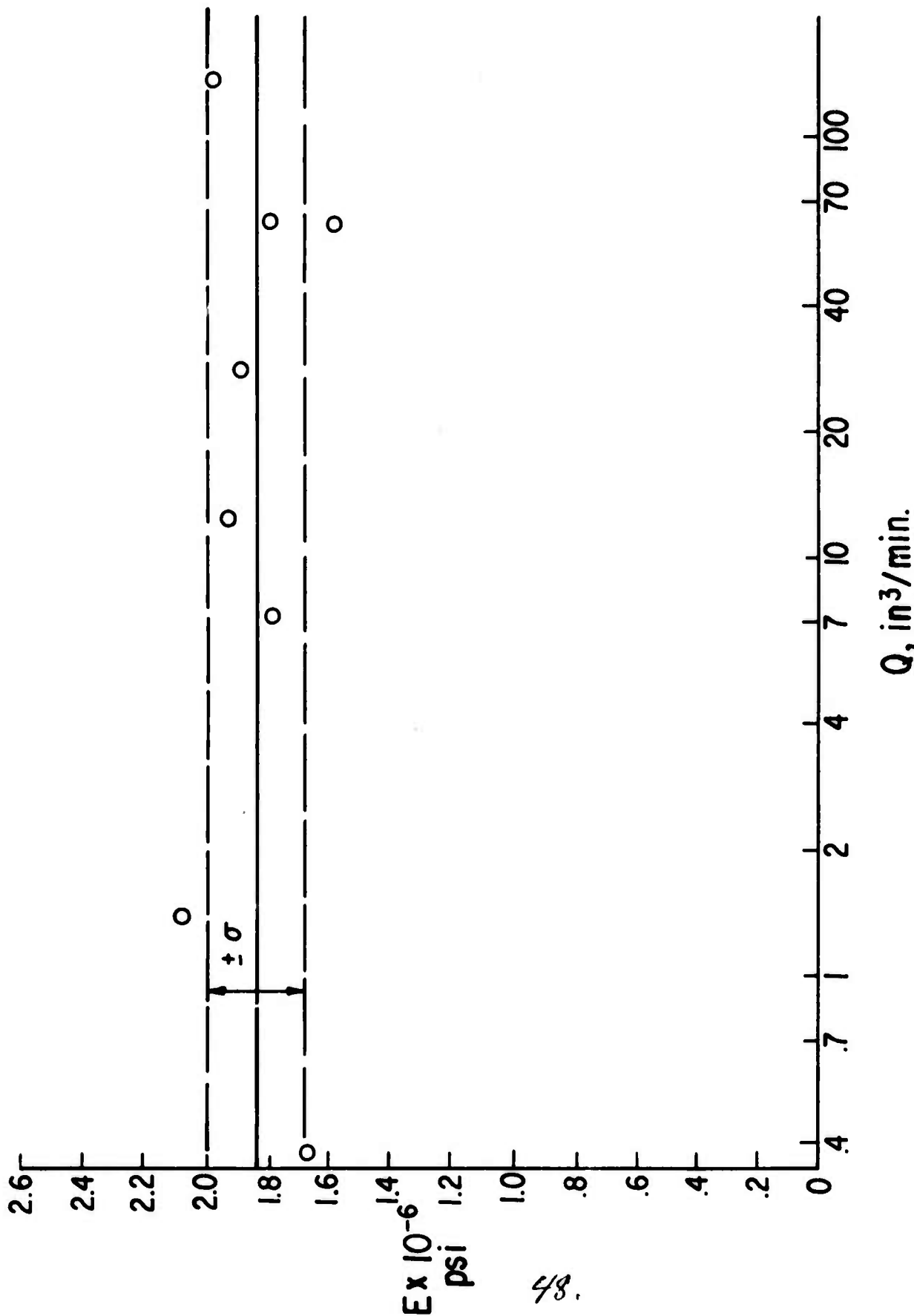
11. Modulus of  $\frac{1}{2}$ " rods;  $A^\circ/A = 6.25$ ,  $\alpha = 6^\circ$ , 40 v/o of  $\frac{1}{8}$ " fibers.



12. Absence of pressure effect on rod stiffness; 1/2" rod,  $A^0/A = 6.25$ ,  $\alpha = 6^\circ$ , 40 v/o of 1/8" fibers.



13. Orientability parameter for a lower fiber concentration with no outflow; 25 v/o 1/8" fiberglass,  $\alpha = 6^\circ$ .



14. Rod stiffness for a lower fiber concentration with no outflow;  
 25 v/o, 1/8" fiberglass,  $\alpha = 6^\circ$ , 3/8" rod ( $A^\circ/A = 11.1$ ).